

Supplementary Materials for

Ultralong room temperature phosphorescence from amorphous organic materials toward confidential information encryption and decryption

Yan Su, Soo Zeng Fiona Phua, Youbing Li, Xianju Zhou, Deblin Jana, Guofeng Liu, Wei Qi Lim, Wee Kong Ong, Chaolong Yang, Yanli Zhao

Published 4 May 2018, *Sci. Adv.* **4**, eaas9732 (2018)
DOI: 10.1126/sciadv.aas9732

The PDF file includes:

- Supplementary Materials and Methods
- fig. S1. Synthetic procedure of compound G.
- fig. S2. Characterization of compound G.
- fig. S3. Fluorescence and phosphorescence spectra of G-doped PVA films.
- fig. S4. Phosphorescence decay profiles of G-doped PVA films.
- fig. S5. Photophysical properties of G-doped PVA films.
- fig. S6. FTIR and Raman spectra of G-doped PVA films.
- fig. S7. ¹H NMR spectra of compounds.
- fig. S8. XPS spectra of the PVA-100-3mg film.
- fig. S9. UV-Vis spectra of the PVA-100-3mg film.
- fig. S10. Thermal properties and XRD patterns of the PVA-100-3mg film.
- fig. S11. SEM images of G-doped PVA films.
- fig. S12. Photophysical properties of the PVA-100-3mg film.
- fig. S13. Temperature-dependent photophysical properties of the PVA-100-3mg film.
- fig. S14. Excitation wavelength-dependent photophysical properties of the PVA-100-3mg film.
- fig. S15. Photophysical properties of G-doped different PVA matrix films.
- fig. S16. Photophysical properties and molecular structures.
- fig. S17. FTIR spectra, XRD patterns, and SEM images of the PVA-100-3mg film under different conditions.
- fig. S18. Phosphorescence emission spectra of patterns for the lotus flower under different conditions.
- fig. S19. Green screen printing procedures without using any inks.

- table S1. Photophysical data of PVA films by doping different concentrations of G.
- table S2. Photophysical data of the PVA-100-3mg film at different irradiation times under a 254-nm UV lamp.
- table S3. Photophysical data of the PVA-100-3mg film at different temperatures.
- table S4. Photophysical data of the PVA-100-3mg film at different excitation wavelengths under ambient conditions.
- Legends for movies S1 to S4
- Reference (38)

Other Supplementary Material for this manuscript includes the following:

(available at advances.sciencemag.org/cgi/content/full/4/5/eaas9732/DC1)

- movie S1 (.avi format). Appearance of the emitting G-doped PVA films when UV light is on and off.
- movie S2 (.avi format). Appearance of the emitting PVA-100-3mg film when UV light is on and off.
- movie S3 (.avi format). Imaging of the logo of the lotus flower.
- movie S4 (.avi format). Imaging of the logo of the lotus flower containing AlQ₃.

Supplementary Materials and Methods

Methods

FTIR spectra were carried out using a Nicolet Is-10(Nicolet) Fourier Transform Infrared Spectrometer. Raman measurements were carried out on a DXR Raman microscope (Thermo Scientific, USA). The excitation laser wavelength was 532 nm. The laser power was set to 10 mW, and 1000 scans with 1 s exposure time were recorded for each spectrum. This configuration was used for all measurements. Differential scanning calorimetry (DSC) was conducted on TA Q20 at a heating rate of 10°C/min under nitrogen. Thermogravimetric analysis (Q500, TGA) was carried out in nitrogen atmosphere from 30 to 650 °C with a ramping rate of 15 °C min⁻¹. X-ray photoelectron spectroscopy measurements were performed on an AXIS Ultra DLD (Kratos, USA) using a monochromatic Al K α X-ray source (anode HT = 15 kV) operated at a vacuum better than 10⁻⁷ Pa. NMR spectra were taken on a DRX-400 MHz (Bruker) superconducting-magnet NMR spectrometer with TMS as an internal standard. UV-vis absorption spectrum was determined on a Shimadzu UV-3600 UV-Vis-NIR spectrophotometer. Fluorescence spectra were carried out on a Varian Cary Eclipse fluorescence spectrophotometer. Persistent room temperature phosphorescent spectra and lifetime were conducted on a Varian Cary Eclipse spectrophotometer, and the samples were measured in the film state. Phosphorescence mode: total decay time 2s; delay time 0.1ms; gate time 500ms. Photoluminescence quantum efficiency was obtained on Edinburgh FLSP920 fluorescence spectrophotometer equipped with an integrating sphere. The photos and supporting videos were recorded by a Canon EOS 80D camera. ICP-MS data were obtained on an ICP-9000(N+M) inductively coupled plasma emission spectrometer. Scanning electron microscope (SEM) images were performed on a JSM-6700F (JEOL) equipped with an energy-dispersive X-ray spectroscopy (EDS) instrument. Powder X-ray diffraction measurements were recorded on a Rigaku D/Max-2500 X-ray diffractometer using Cu K α radiation with 2 θ range of 2-50°, 40 KeV, and 30 mA having a scanning rate of 0.01° s⁻¹ (2 θ) at room temperature.

Optical energy band gap (E_g) calculation

Using the UV-vis spectra, the optical energy band gap was calculated by Tauc's expression

$$\alpha h\nu = \beta(h\nu - E_g)^n \quad (1)$$

The absorption coefficient (α) of fabricated films was determined from the absorbance (A) values after the correction for reflection using the equation

$$\alpha = \frac{2.303}{d} \log \frac{I}{I_0} = \left(\frac{2.303}{d}\right)A \quad (2)$$

where A is the absorbance, d is the film thickness, h is Planck's constant, ν is the frequency of

the incident photons, β is a constant, E_g is the optical energy band gap, and the exponent (n) is an empirical index that depends on the nature of electronic transition responsible for the absorption (1/2, 3/2, 2, and 3 for direct allowed, direct forbidden, indirect allowed, and indirect forbidden transitions, respectively)(32,38). The dependence of $(\alpha hv)^{1/n}$ and photon energy (hv) was plotted for materials using different values of n , and the best fit was obtained for $n = 2$. It was shown that the transition process is indirect in K -space and that interactions with photons are feasible. The values of optical band gap E_g for films can be obtained from the extrapolation of linear portions of these plots with the energy axis ($(\alpha hv)^{1/2} = 0$) of the plots of $(\alpha hv)^{1/2}$ versus hv at room temperature.

Synthesis of methyl 4-hydroxybenzoate. 4-Hydroxy benzoic acid (35 mmol, 5.3 g) and MeOH (80 mL) were loaded into a 150 mL round bottom flask fitted with a reflux condenser. Concentrated sulfuric acid (2.5 mL) was added as a catalyst and the contents were refluxed for 12 h. The reaction mixture was cooled down to room temperature and excess MeOH was removed using a rotary evaporator. The residue obtained was dissolved in chloroform and washed thoroughly with 10% sodium bicarbonate solution. The organic layer was dried over anhydrous $MgSO_4$ and concentrated to give the product in 95% yield. 1H NMR (400 Hz, $CDCl_3$, ppm): δ 7.973–7.951 (d, 2H, Ar-H), 6.887–6.865 (d, 2H, Ar-OH), 5.8 (s, 1H, Ar-OH), 3.896 (s, 3H, $COOCH_3$).

Hexa-(3,5-carboxyl-phenoxy)-cyclotriphosphazene (G1), hexa-(2-carboxyl-phenoxy)-cyclotriphosphazene (G3), and hexa-(3-carboxyl-phenoxy)-cyclotriphosphazene (G4) were synthesized according to a similar procedure of CTP-COOH.

Hexa-(3,5-carboxyl-phenoxy)-cyclotriphosphazene (G1): 1H NMR (400 MHz, $DMSO-d_6$, ppm): δ 13.28 (s, 12H, -COOH), 8.23 (s, 6H, Ar-H), 7.79 (s, 12H, Ar-H). ^{13}C NMR (300 MHz, $DMSO-d_6$, ppm): δ 169.98, 150.06, 134.97, 124.50. ESI-MS: 1244.07 (G1 + Na^+).

Hexa-(2-carboxyl-phenoxy)-cyclotriphosphazene (G3): 1H NMR (400 MHz, $DMSO-d_6$, ppm): δ 13.09 (s, 6H, -COOH), 7.81-7.79 (d, 6H, Ar-H), 7.21-7.14 (t, 12H, Ar-H), 6.96-6.89 (d, 6H, Ar-H). ^{13}C NMR (300 MHz, $DMSO-d_6$, ppm): δ 172.40, 166.26, 136.08, 119.08, 117.52. ESI-MS: 958.08 (G3 + H^+).

Hexa-(3-carboxyl-phenoxy)-cyclotriphosphazene (G4): 1H NMR (400 MHz, $DMSO-d_6$, ppm): δ 13.13 (s, 6H, -COOH), 7.79-7.77 (d, 6H, Ar-H), 7.64 (s, 6H, Ar-H), 7.39-7.35 (t, 6H, Ar-H), 7.13-1.11 (d, 6H, Ar-H). ^{13}C NMR (300 MHz, $DMSO-d_6$, ppm): δ 166.60, 150.07, 133.14, 130.50, 126.89, 125.09, 121.50. ESI-MS: 958.09 (G4 + H^+).

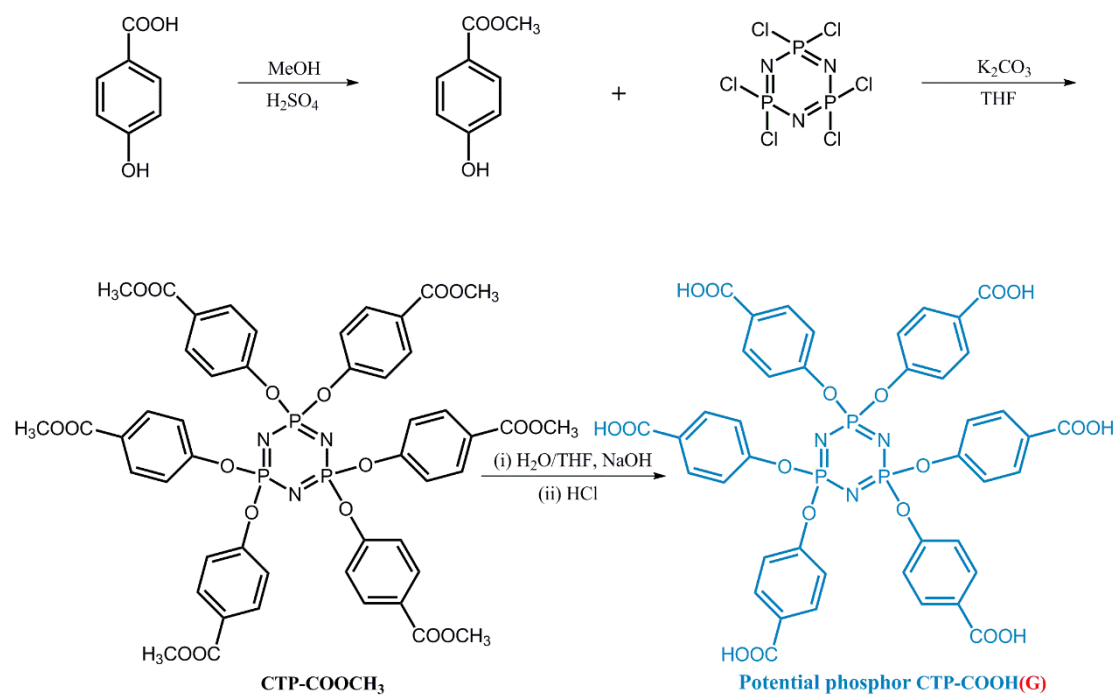


fig. S1. Synthetic procedure of compound G.

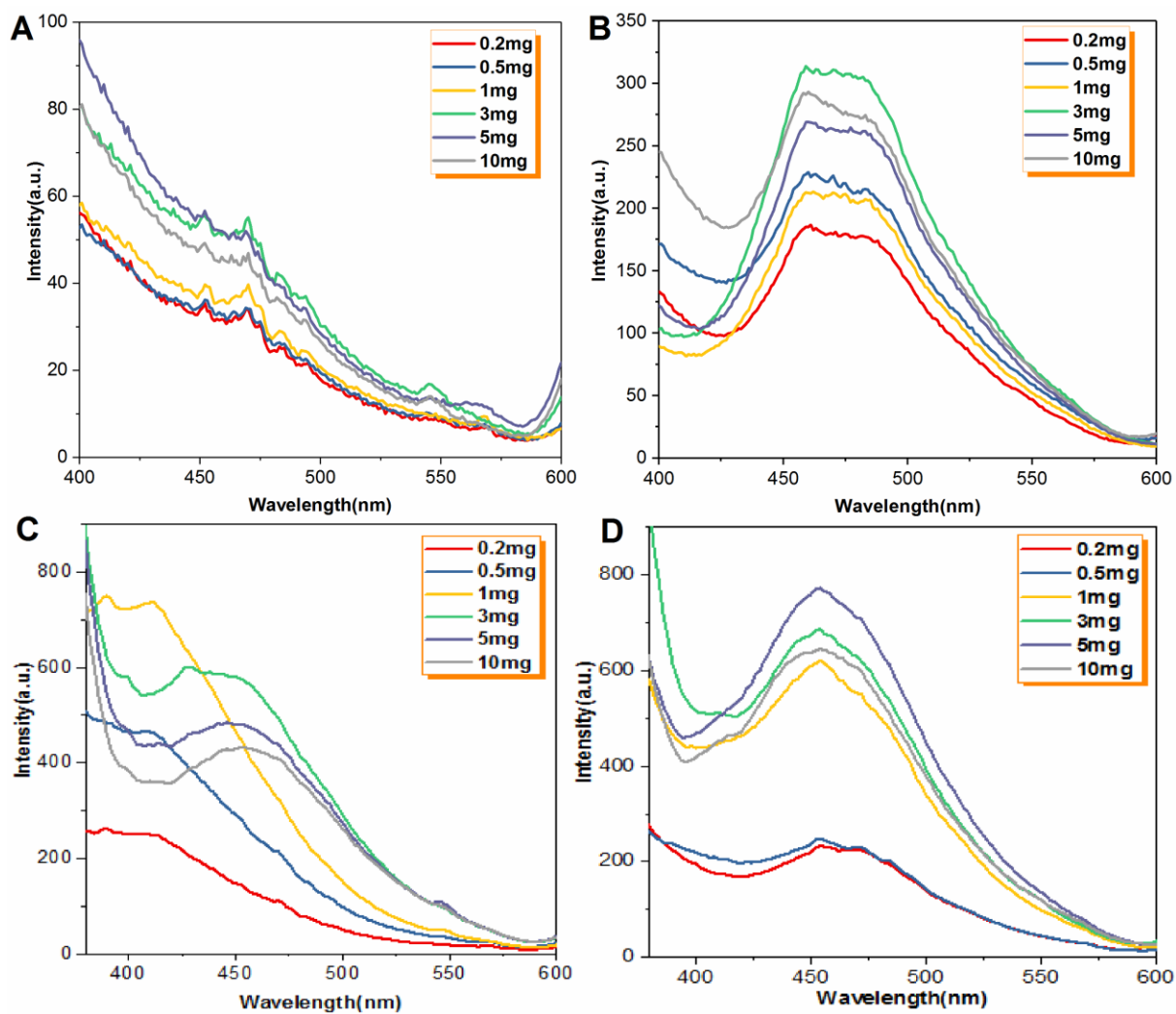


fig. S3. Fluorescence and phosphorescence spectra of G-doped PVA films. Fluorescence spectra of PVA-100 films doped with different concentrations of G at 298 K (A) without 254 nm UV irradiation, and (B) with 254 nm UV irradiation for 65 min (λ_{ex} and λ_{em} slit: 5nm and 5nm; λ_{ex} : 280 nm). Phosphorous spectra of PVA-100 films doped with different concentrations of G at 77 K (C) without 254 nm UV irradiation, and (D) with 254 nm UV irradiation for 65 min (λ_{ex} and λ_{em} slit: 5nm and 5nm; λ_{ex} : 280 nm).

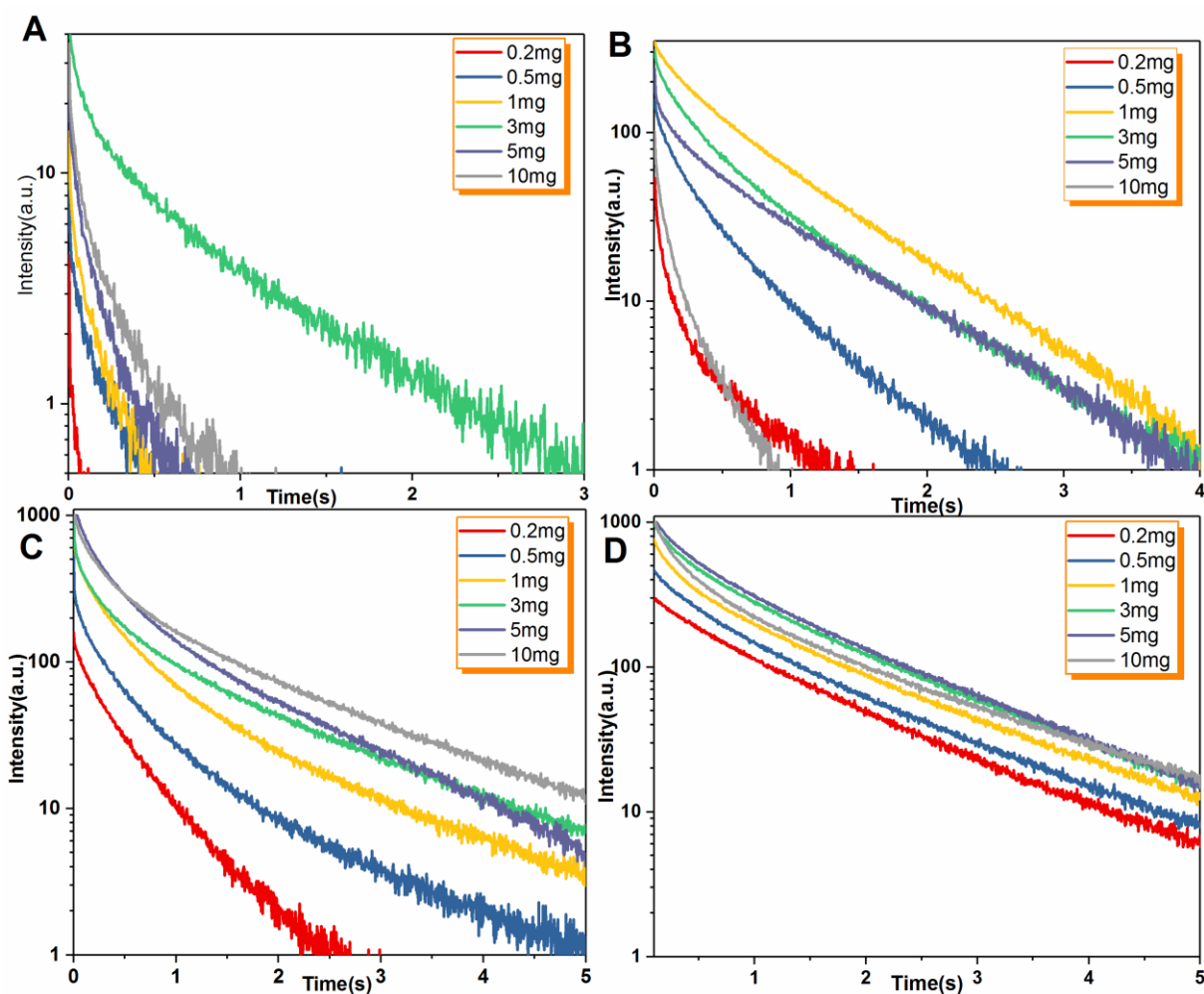


fig. S4. Phosphorescence decay profiles of G-doped PVA films. Phosphorescence decay profiles of PVA-100 films doped with different concentrations of G (**A**) without 254 nm UV irradiation at 298 K, (**B**) with 254 nm UV irradiation for 65 min at 298 K, (**C**) without 254 nm UV irradiation at 77 K, and (**D**) with 254 nm UV irradiation for 65 min at 77 K (monitored wavelength: 480 nm; λ_{ex} and λ_{em} slit: 5nm and 5nm, λ_{ex} : 280 nm).

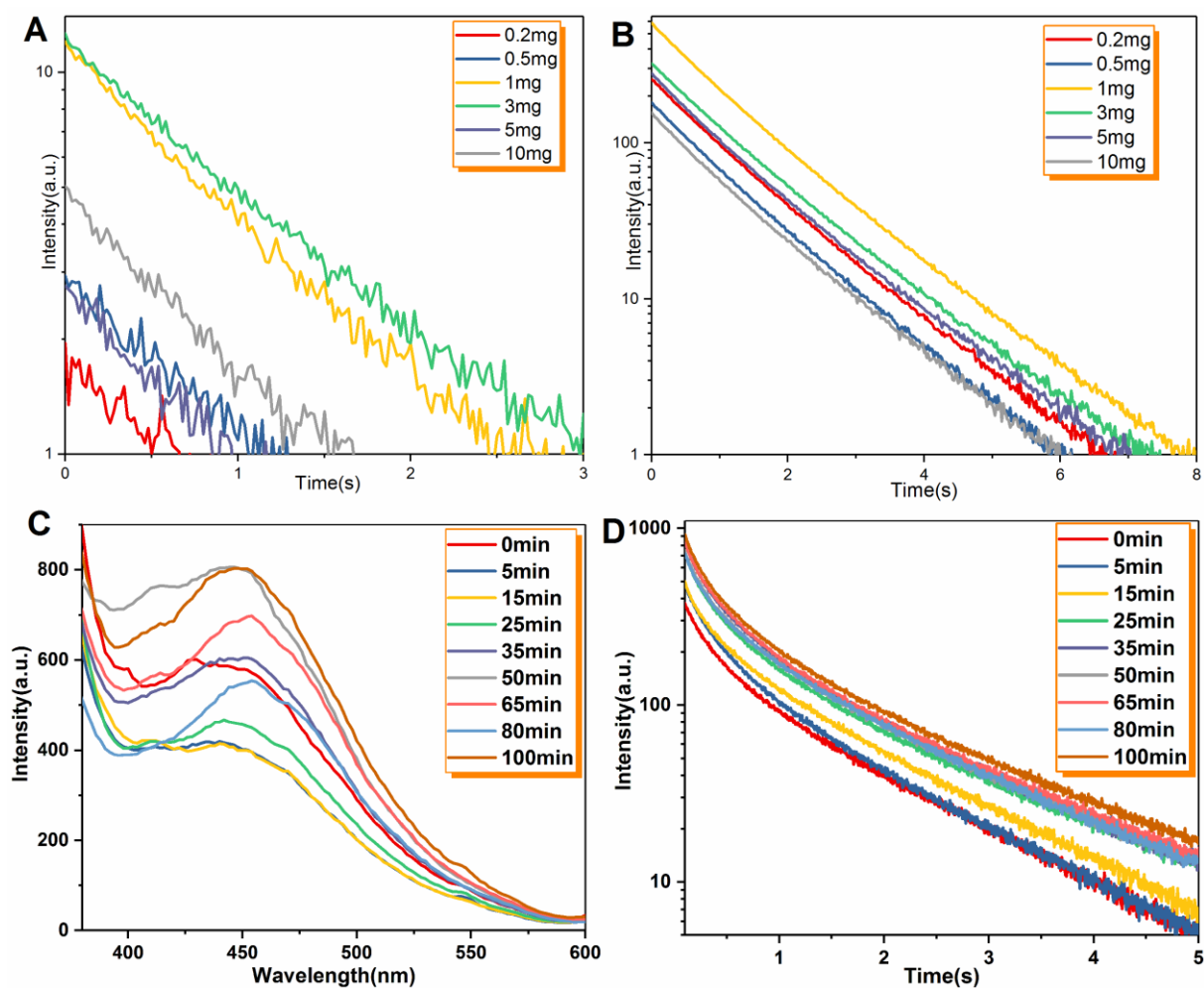


fig. S5. Photophysical properties of G-doped PVA films. Time-dependent luminescent spectra of PVA-100 films doped with different concentrations of G after turning off the UV light (delayed time: *c.a.* 50 ms) at 298 K: (A) without 254 nm UV irradiation, and (B) with 254 nm UV irradiation for 65 min (λ_{ex} and λ_{em} slit: 5nm and 5nm; λ_{ex} : 280 nm; λ_{em} : 480 nm). (C) Phosphorescent spectra of PVA-100-3mg film upon different irradiation time by 254 nm lamp at 77K. (D) Amorphous organic URTP decay profiles of PVA-100-3mg film upon different irradiation time by 254 nm UV lamp at 77K.

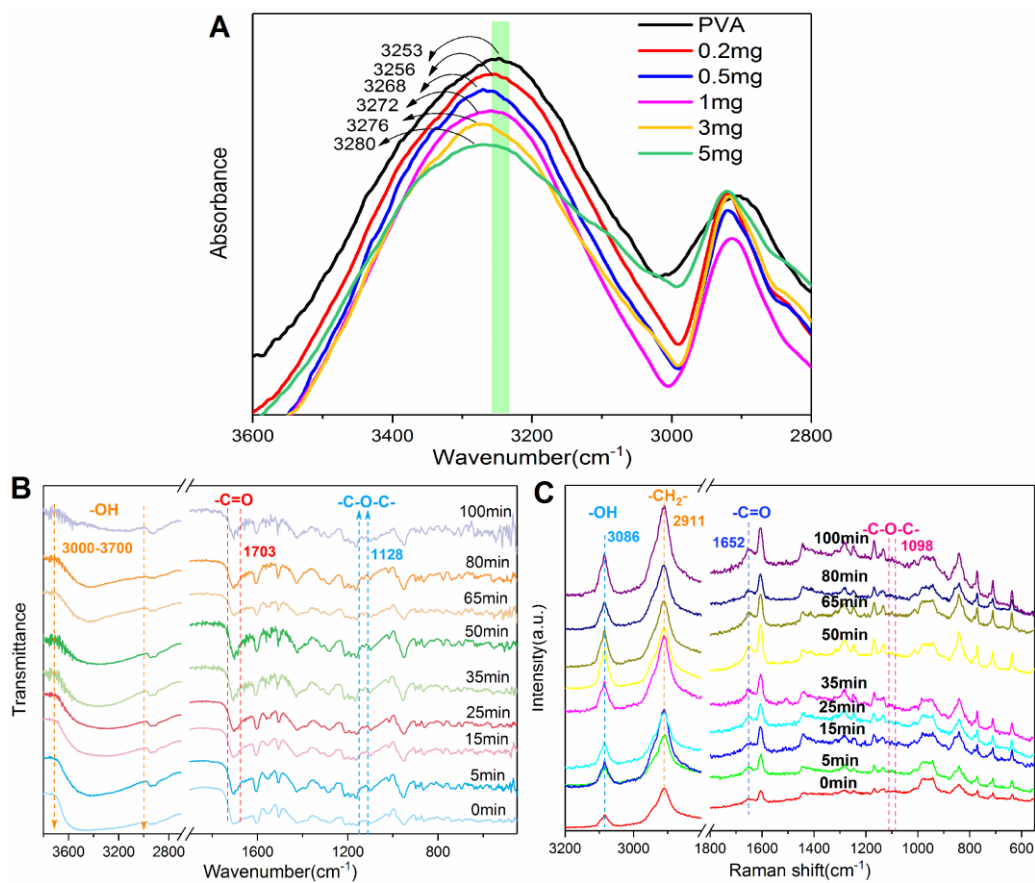


fig. S6. FTIR and Raman spectra of G-doped PVA films. (A) Stretching vibrations of O-H groups ($\nu_{\text{O-H}}$) in FT-IR spectra for PVA and G-doped PVA films. (B) FT-IR spectra and (C) Raman spectra of PVA-100-3mg upon different irradiation time by 254 nm UV light.

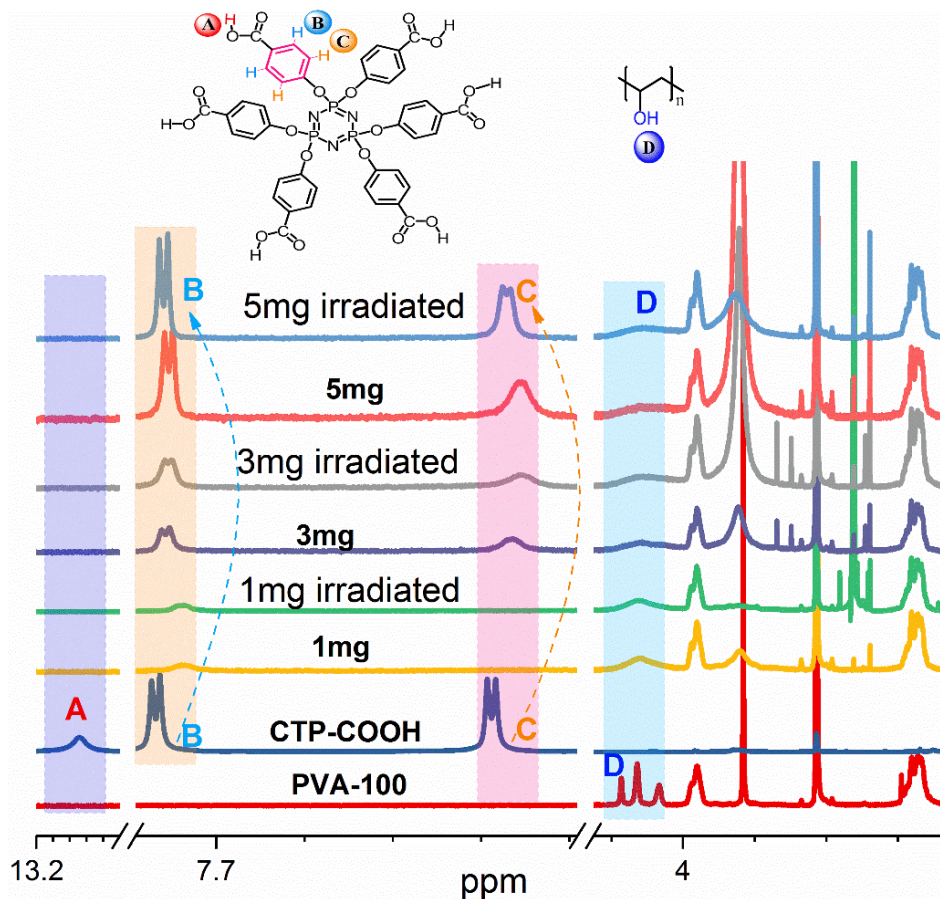


fig. S7. ¹H NMR spectra of compounds. ¹H NMR spectra of PVA-100, compound G, and G-doped PVA films (without or with 254nm UV irradiation for 65 min) doped with different concentrations of G. Inset shows chemical structures of compound G (left) and PVA-100 (right).

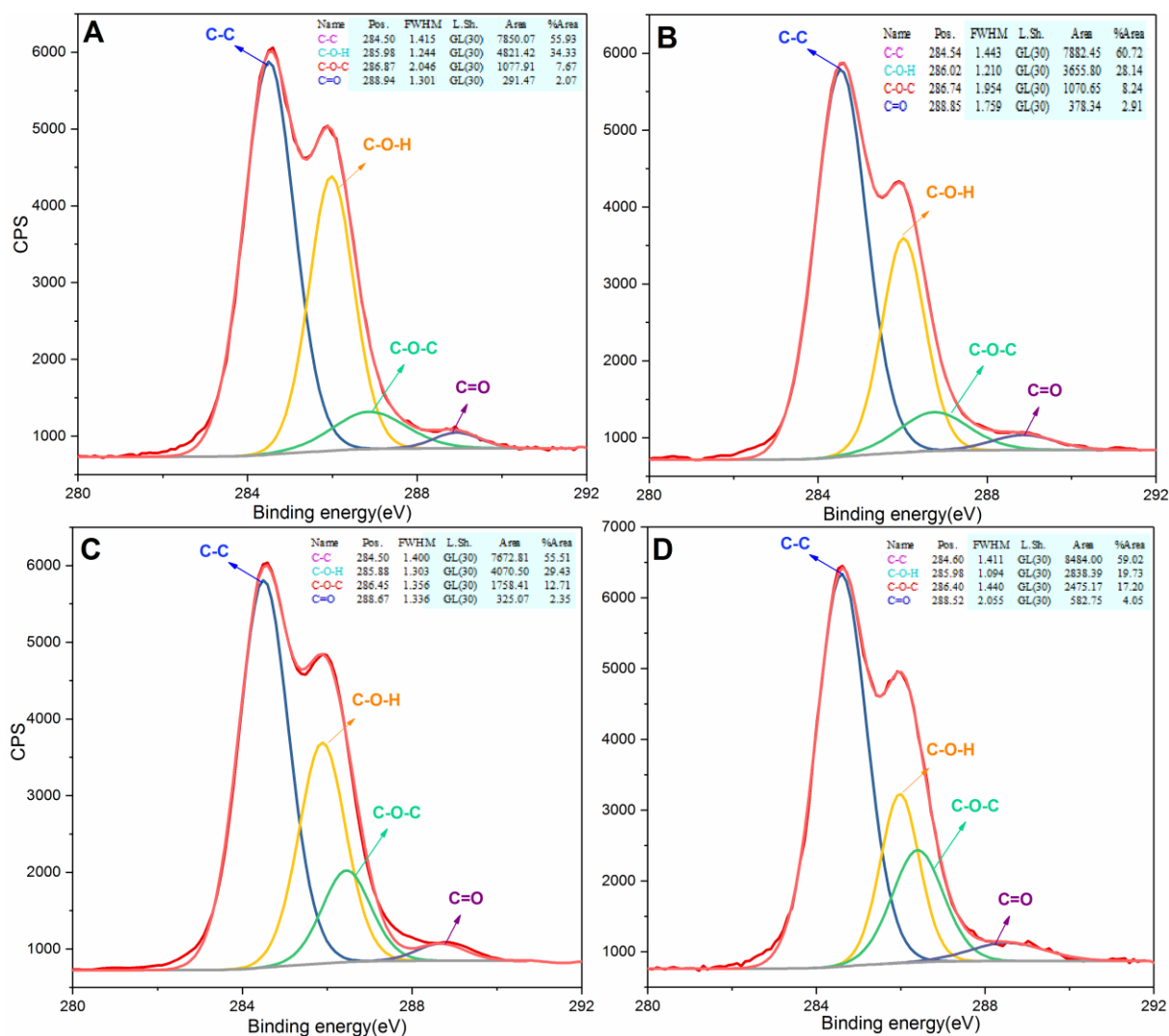


fig. S8. XPS spectra of the PVA-100-3mg film. High resolution XPS spectra of PVA-100-3mg film upon different irradiation time by 254 nm UV light for (A) 0 min, (B) 15 min, (C) 65 min, and (D) 100 min.

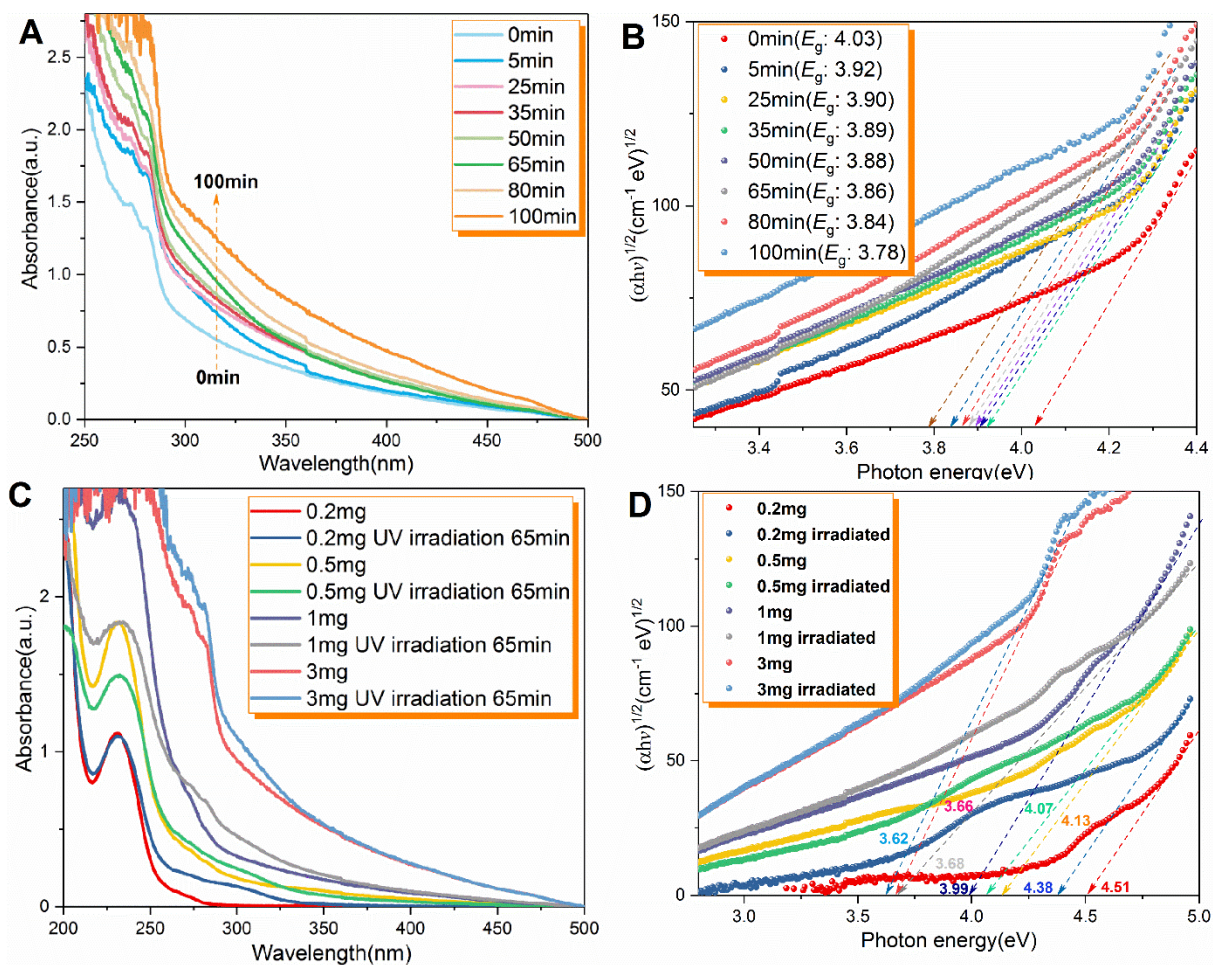


fig. S9. UV-Vis spectra of the PVA-100-3mg film. (A) UV-vis spectra of PVA-100-3mg film upon different irradiation time by 254 nm UV lamp. (B) Tauc's plots for the determination of directed band gaps for PVA-100-3mg film upon different irradiation time. (C) UV-vis spectra of PVA films (without or with 254 nm UV irradiation for 65min) containing different concentrations of G. (D) Tauc's plots for the determination of directed band gaps for PVA films (without or with 254 nm UV irradiation for 65min) containing different concentrations of G.

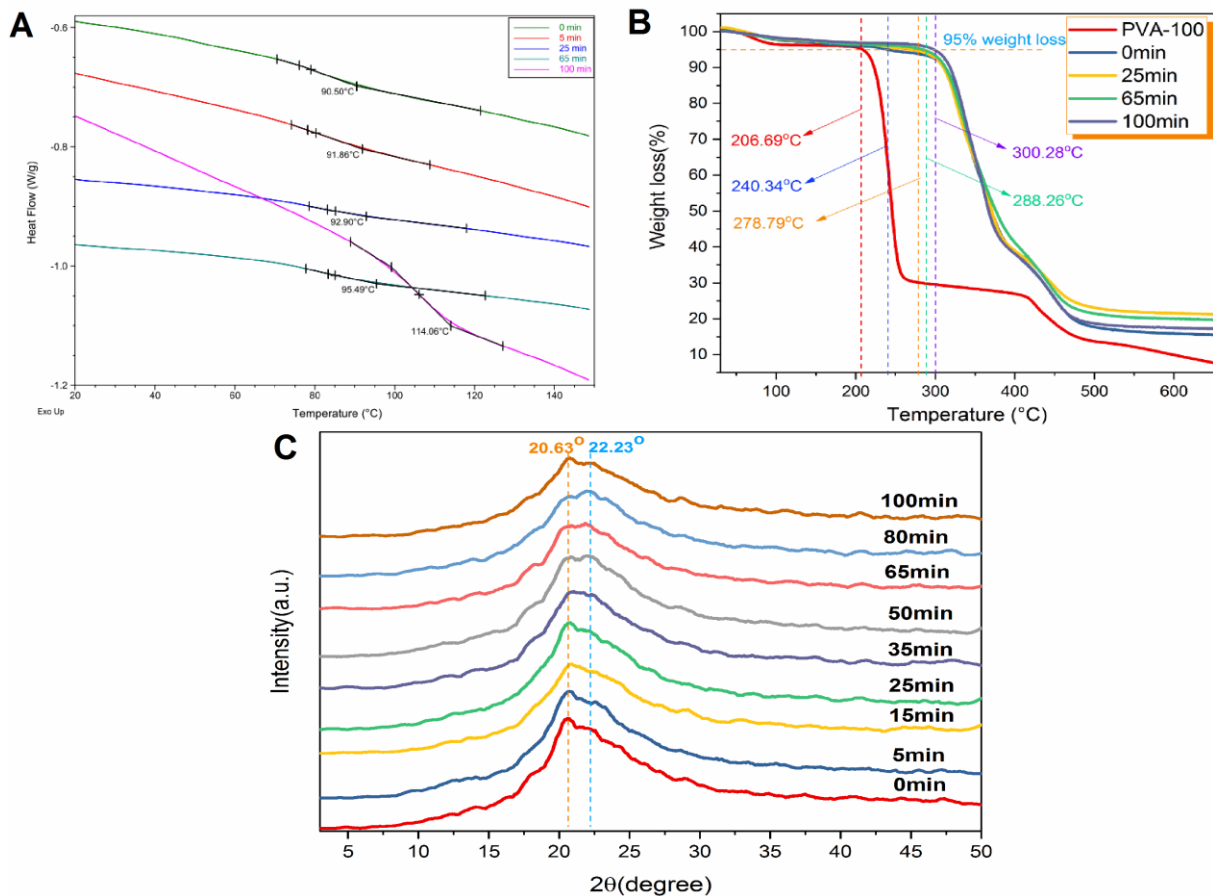


fig. S10. Thermal properties and XRD patterns of the PVA-100-3mg film. (A) DSC curves of PVA-100-3mg film under different irradiation time by 254 nm UV lamp. (B) TGA curves of PVA-100 and G-doped PVA films upon different irradiation time by 254 nm UV lamp. (C) Powder XRD patterns of PVA-100-3mg film upon different irradiation time by 254 nm UV lamp.

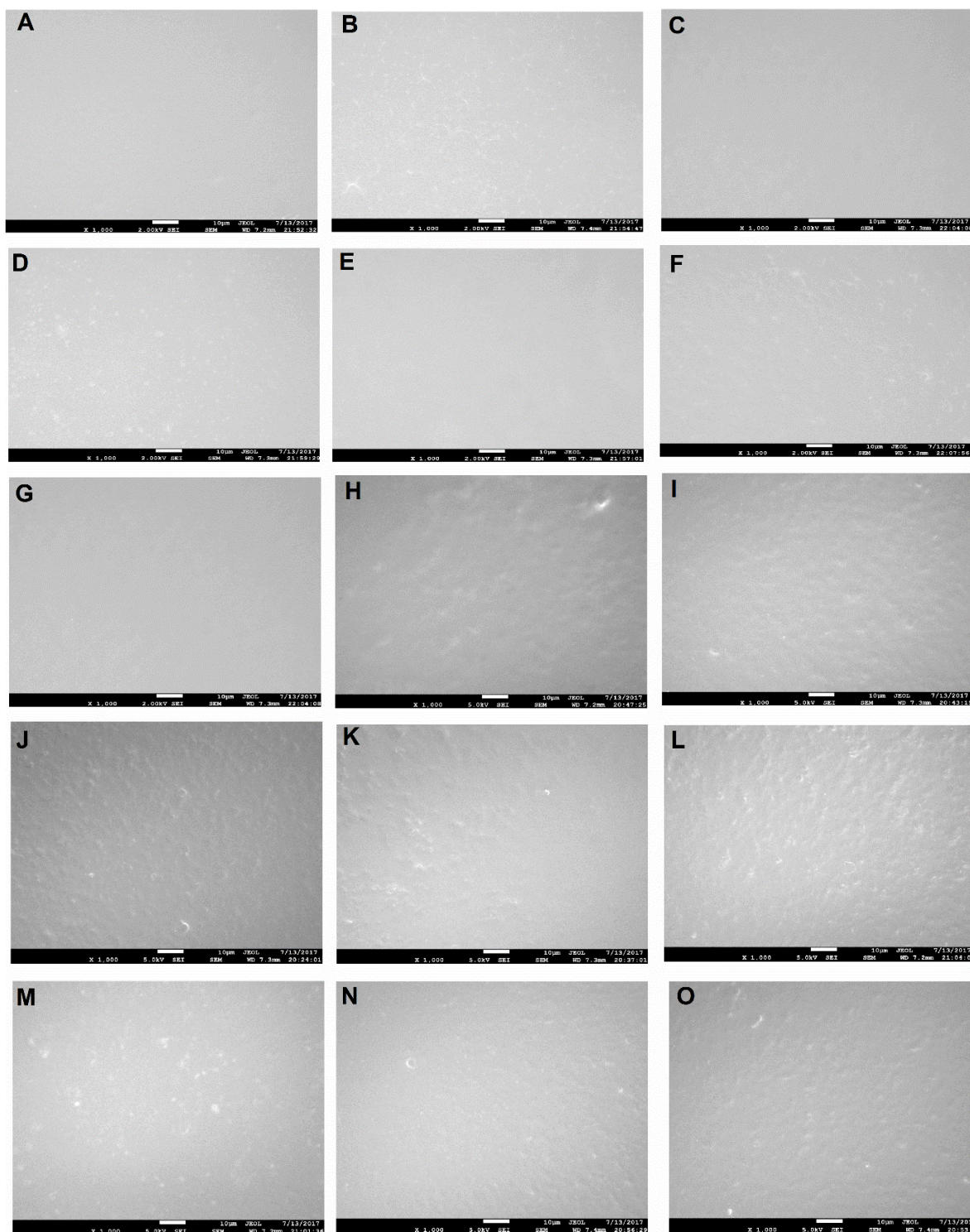


fig. S11. SEM images of G-doped PVA films. SEM images of PVA films containing different concentrations of G. (A) PVA-100-0.5mg film without UV irradiation. (B) PVA-100-0.5mg film with 254 nm UV irradiation for 65 min. (C) PVA-100-1mg film without UV irradiation. (D) PVA-100-1mg film with 254 nm UV irradiation for 65 min. (E) PVA-100-3mg film without UV irradiation. (F) PVA-100-3mg film with 254 nm UV irradiation for 65min. SEM images of PVA-100-3mg film upon different irradiation time by 254 nm UV lamp for (G) 0 min, (H) 5 min, (I) 15 min, (J) 25 min, (K) 35 min, (L) 50 min, (M) 65 min, (N) 80 min, and (O) 100 min.

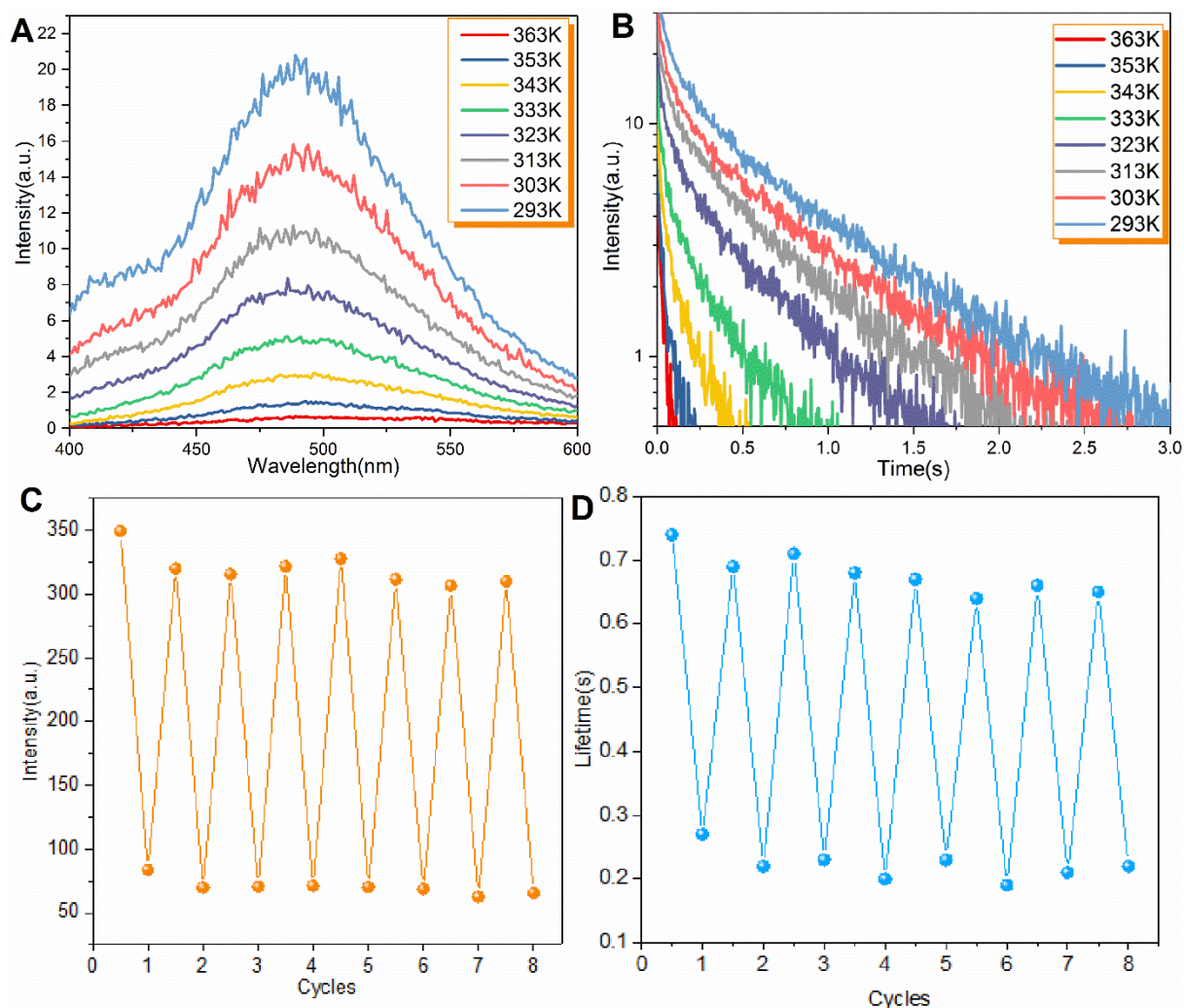


fig. S12. Photophysical properties of the PVA-100-3mg film. (A) Phosphorescent spectra of unirradiated PVA-100-3mg film at different temperature (λ_{ex} : 280 nm). (B) Phosphorescent decay profiles of unirradiated PVA-100-3mg film at different temperature (λ_{ex} : 280 nm; λ_{em} : 480 nm). (C) *In situ* phosphorescence intensity of PVA-100-3mg film at 480 nm for eight cycles (λ_{ex} : 280nm). (D) *In situ* phosphorescence lifetime of PVA-100-3mg film for eight cycles (λ_{ex} : 280nm, λ_{em} : 480nm).

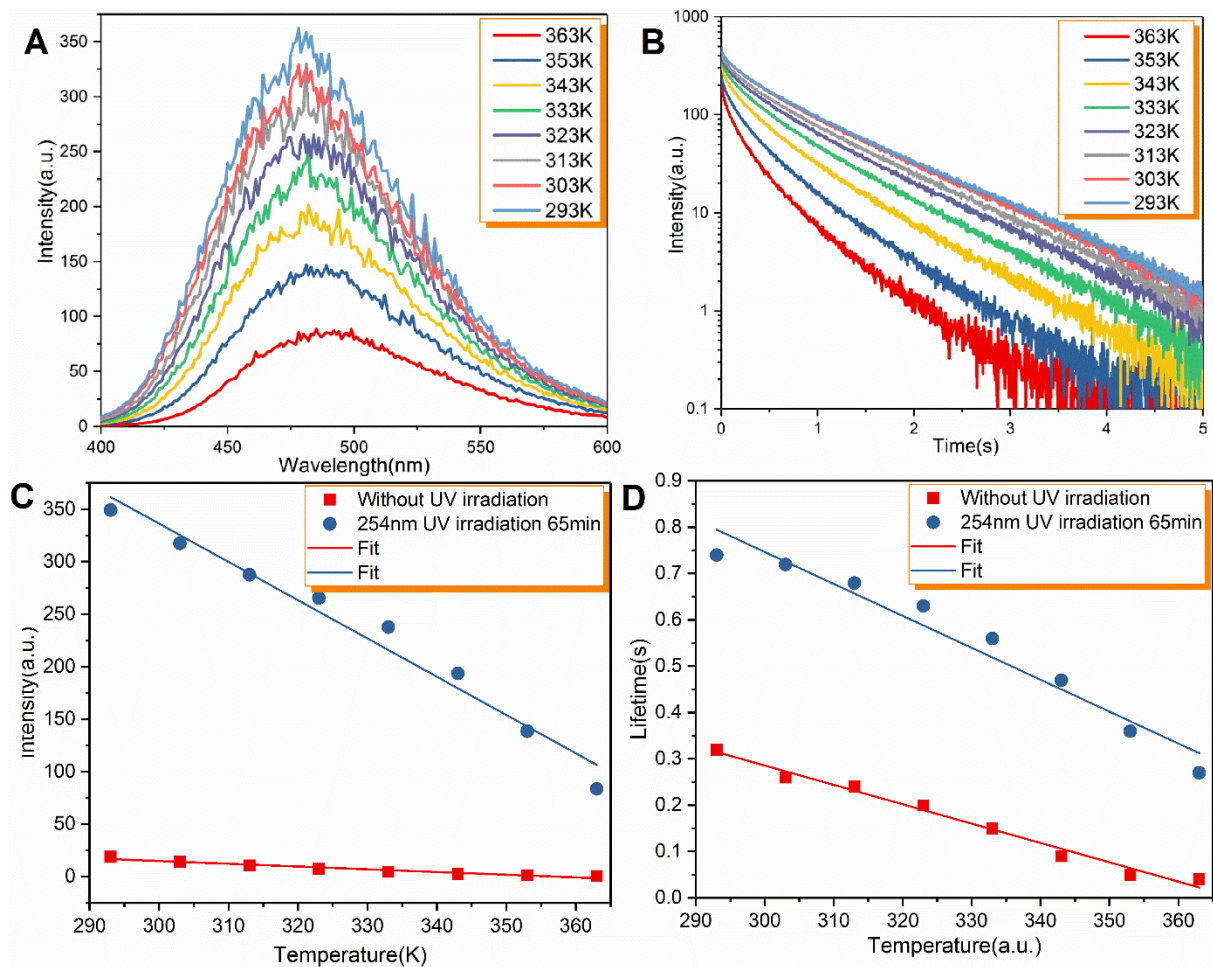


fig. S13. Temperature-dependent photophysical properties of the PVA-100-3mg film. (A) Phosphorescent spectra of PVA-100-3mg film at different temperature (λ_{ex} : 280 nm). (B) Phosphorescent decay profiles of PVA-100-3mg film at different temperature (monitored: 480 nm, λ_{ex} : 280 nm). (C) Plots of phosphorescent intensity vs temperature for unirradiated/irradiated PVA-100-3mg films. (D) Plots of phosphorescent lifetime vs temperature for unirradiated/irradiated PVA-100-3mg films.

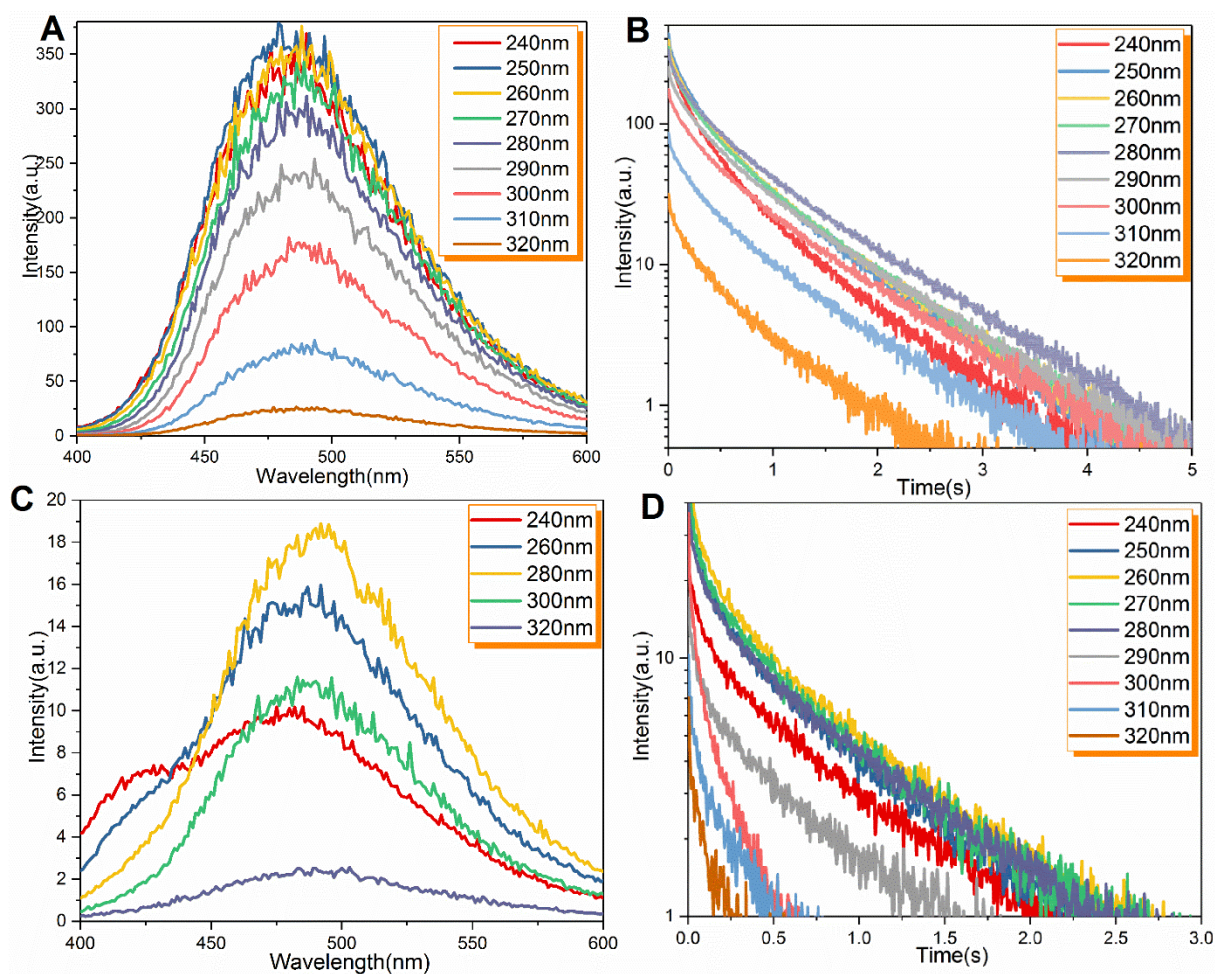


fig. S14. Excitation wavelength–dependent photophysical properties of the PVA-100-3mg film. (A) Phosphorescent spectra of PVA-100-3mg film under different excitation wavelengths at 298K. (B) Phosphorescent decay profiles of PVA-100-3mg film under different excitation wavelengths at 298K (monitored at 480 nm). (C) Phosphorescent spectra of unirradiated PVA-100-3mg film under different excitation wavelengths at 298K. (D) Phosphorescent decay profiles of unirradiated PVA-100-3mg film under different excitation wavelengths at 298K (monitored at 480 nm).

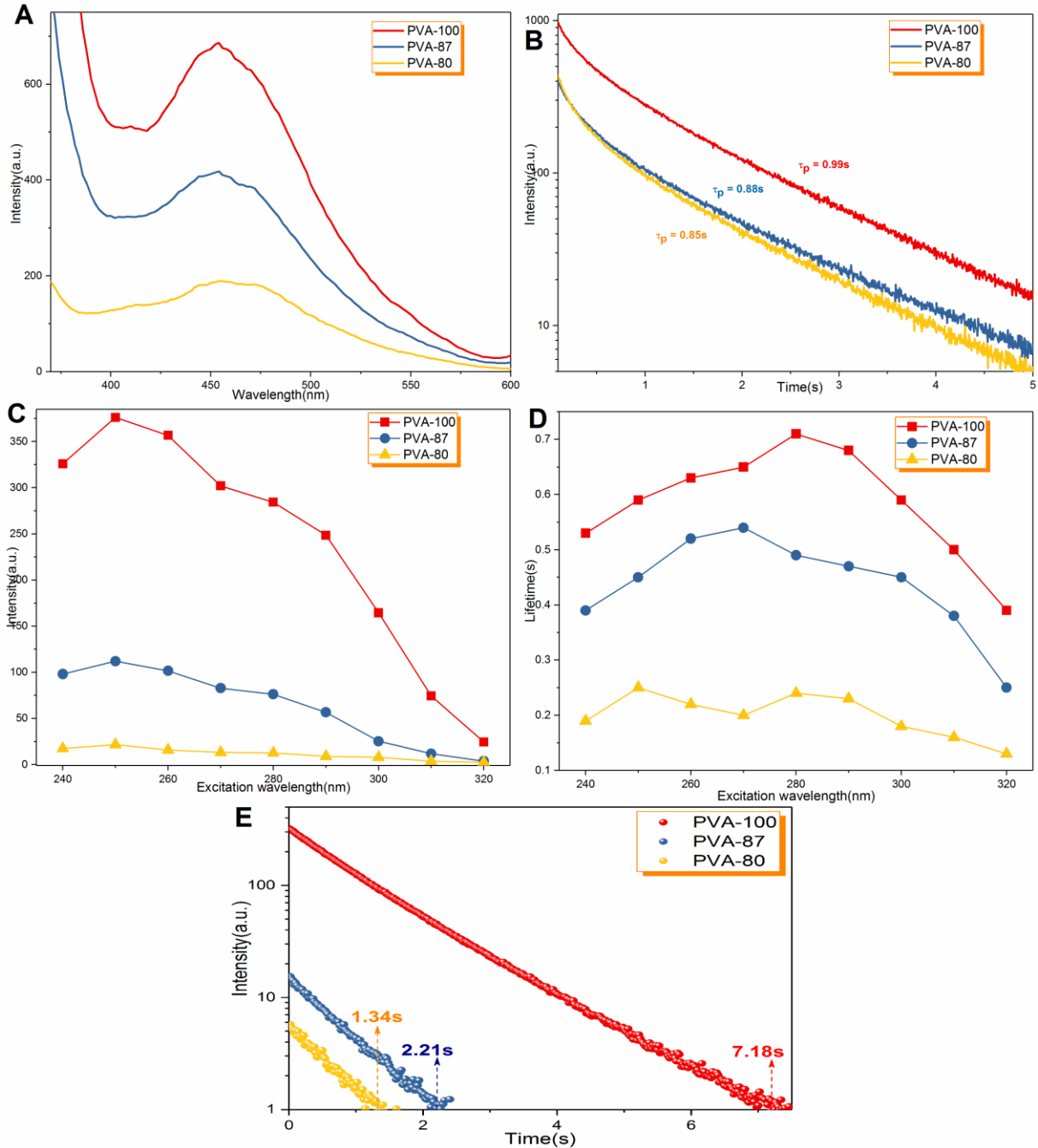


fig. S15. Photophysical properties of G-doped different PVA matrix films. (A)

Phosphorescent spectra of PVA-100-3mg, PVA-87-3mg and PVA-80-3mg films at 77 K. **(B)**

Phosphorescent decay profiles of PVA-100-3mg, PVA-87-3mg and PVA-80-3mg films at 77 K

(monitored: 480nm, λ_{ex} : 280nm). **(C)** Phosphorescent intensity of PVA-100-3mg,

PVA-87-3mg and PVA-80-3mg films at 480 nm under different excitation wavelengths at 298

K. **(D)** Phosphorescent lifetime of PVA-100-3mg, PVA-87-3mg and PVA-80-3mg films under

different excitation wavelengths at 298 K (monitored: 480 nm, λ_{ex} : 280 nm). **(E)**

Time-dependent ultralong luminescent spectra of irradiated PVA-100-3mg, PVA-87-3mg and PVA-80-3mg films (delayed time: *c.a.* 50 ms) at 298 K (λ_{ex} : 280 nm, λ_{em} : 480 nm).

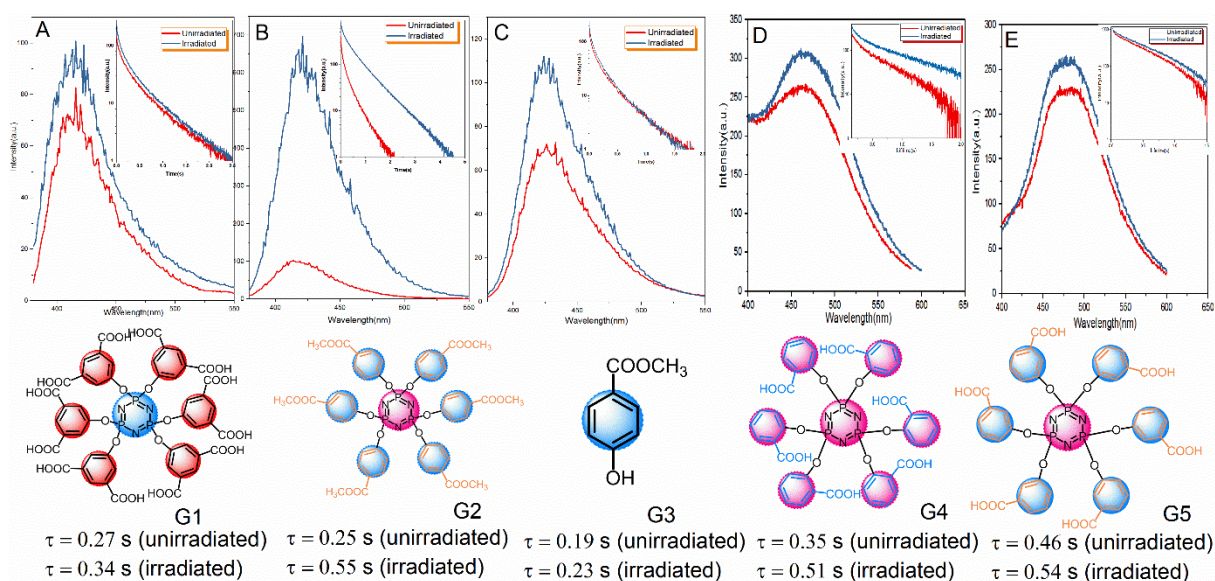


fig. S16. Photophysical properties and molecular structures. Phosphorescent spectra of phosphor-doped PVA films and chemical structures of these potential phosphors. Inset shows phosphorescent decay profiles of phosphor-doped PVA films. **(A)** G1-doped PVA film. **(B)** G2-doped PVA film. **(C)** G3-doped PVA film. **(D)** G4-doped PVA film. **(E)** G5-doped PVA film.

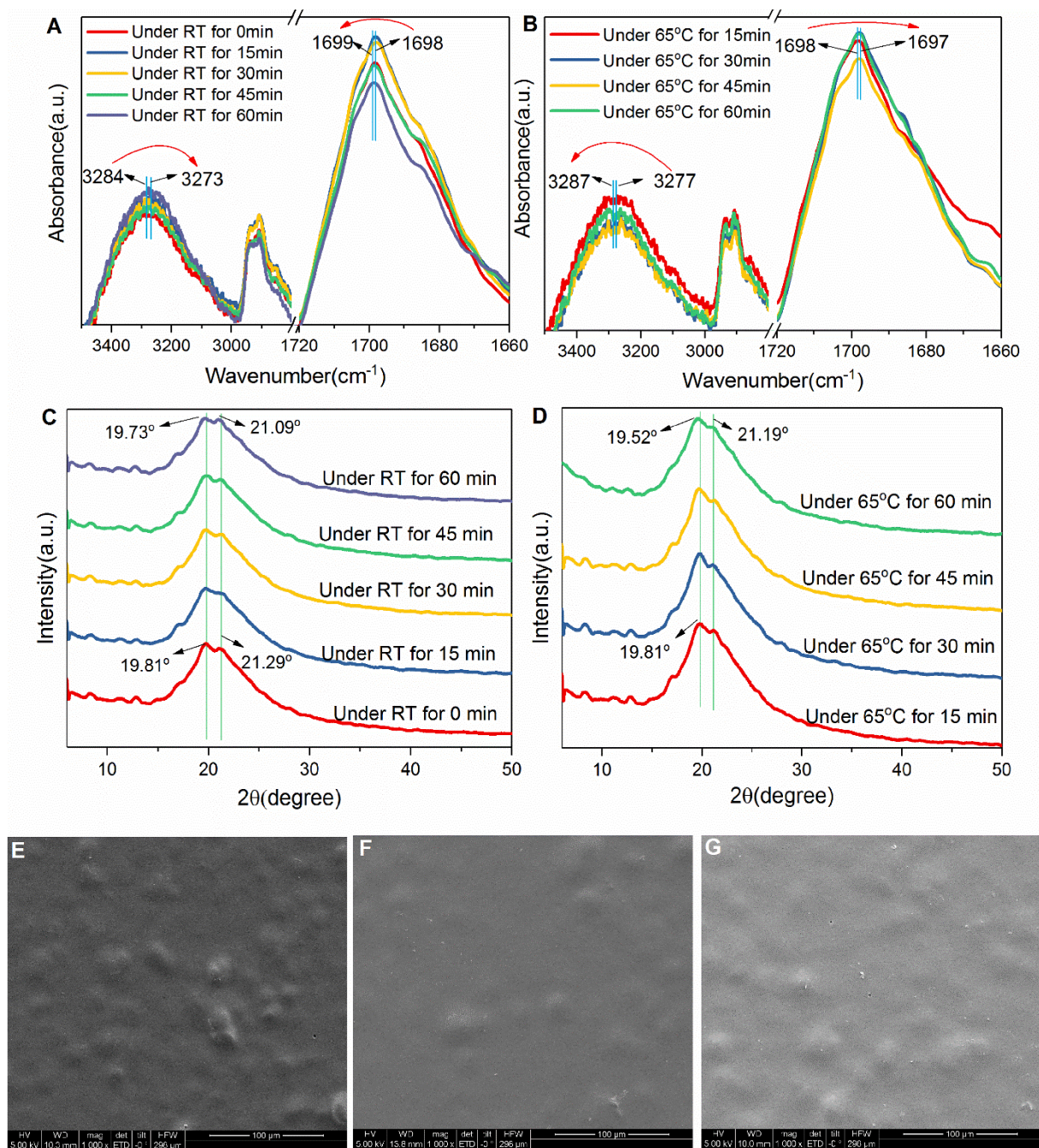


fig. S17. FTIR spectra, XRD patterns, and SEM images of the PVA-100-3mg film under different conditions. FT-IR spectra (A) under room temperature for different times and (B) under 65 °C for different times. Powder XRD patterns (C) under room temperature for different times and (D) under 65°C for different times. SEM images under room temperature (E) for 0 min and (F) for 60 min. (G) SEM image after incubation at 65 °C for 60 min.

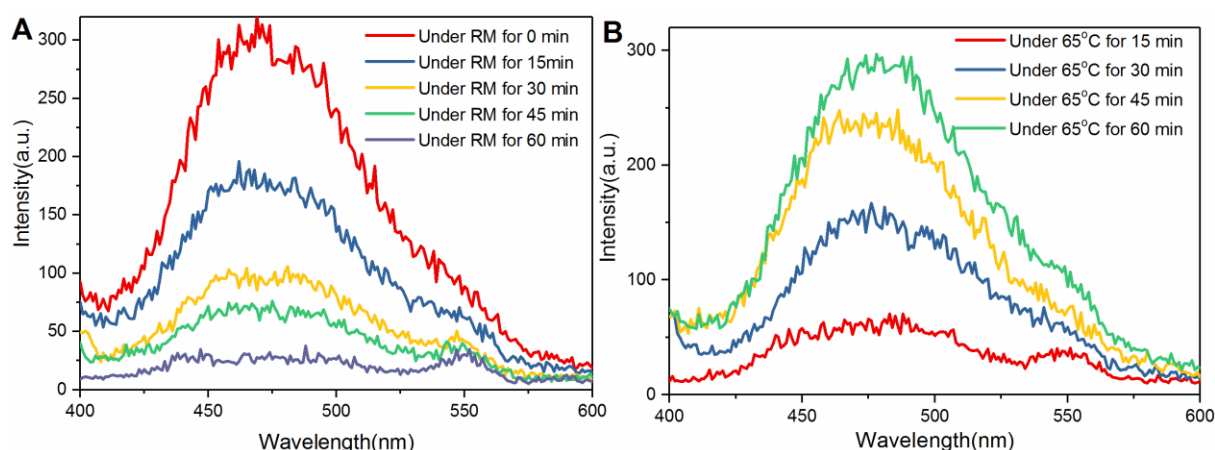


fig. S18. Phosphorescence emission spectra of patterns for the lotus flower under different conditions. (A) Under room temperature (RT) for different time. (B) Incubation at 65 °C for different time.

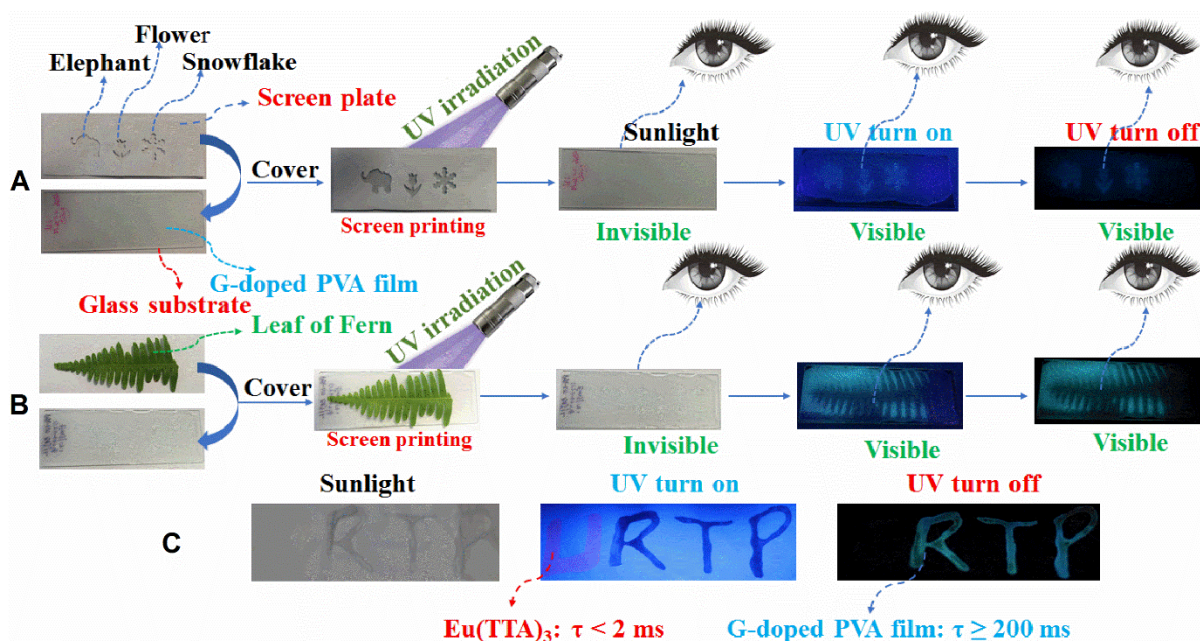


fig. S19. Green screen printing procedures without using any inks. Screen printing procedures using a home-made paper with (A) cartoon patterns (elephant, flower, and snowflake) and (B) fern leaf as screen plate. (C) Four letters (URTP) on common printing paper imaging under sunlight and 254 UV lamp, as well as after the removal of excitation source. The letter “U” was written utilizing a common rare-earth complex $\text{Eu}(\text{TTA})_3$ in THF, and the other three letters “RTP” were written using our G-doped PVA aqueous solution.

table S1. Photophysical data of PVA films by doping different concentrations of G.

System	I_p (RT) ^a		I_p (77K) ^b		I_f (RT) ^c		t (s) ^d		τ_p/s (RT) ^e		τ_p/s (77K) ^f		Φ_p (RT) ^g	
	UID ^h	ID ⁱ	UID	ID	UID	ID	UID	ID	UID	ID	UID	ID	UID	ID
0.2 mg	0.39	22.83	253.19	232.77	33.90	185.18	0.68	6.52	0.04	0.31	0.36	0.91	1.03%	4.26%
0.5 mg	2.70	143.84	467.86	250.79	34.31	227.21	1.19	6.04	0.10	0.37	0.51	0.94	1.12%	6.44%
1 mg	5.84	249.69	739.39	620.61	38.36	212.72	2.63	7.76	0.13	0.75	0.56	0.97	2.36%	9.18%
3 mg	19.51	315.47	584.05	687.74	54.32	313.79	3.06	7.18	0.28	0.71	0.68	0.99	2.85%	11.23%
5 mg	11.86	175.09	482.46	775.69	51.99	269.07	0.97	6.91	0.15	0.69	0.73	1.01	1.62%	5.51%
10 mg	13.53	35.39	432.14	644.23	44.97	290.94	1.67	5.94	0.17	0.23	0.81	0.89	1.27%	3.09%

^a Phosphorescent intensity at room temperature; ^b Phosphorescent intensity at 77K; ^c Fluorescent intensity at room temperature; ^d Time of ultralong luminescent intensity at 1 a.u.; ^e Phosphorescent lifetime at room temperature; ^f Phosphorescent lifetime at 77K; ^g Phosphorescent quantum yield (Φ_p) at room temperature; ^h Without 254 nm UV irradiation; ⁱ Under 254 nm UV irradiation for 65 min. UID: unirradiated, ID: irradiated.

table S2. Photophysical data of the PVA-100-3mg film at different irradiation times under a 254-nm UV lamp.

System		0min	5min	15min	25min	35min	50min	65min	80min	100min
τ_p (s) ^a	298 K	0.28	0.36	0.41	0.44	0.5	0.67	0.71	0.64	0.59
	77 K	0.68	0.74	0.79	0.81	0.82	0.86	0.88	0.84	0.91
Φ_p ^b	298 K	2.85%	3.19%	4.24%	4.83%	6.28%	9.31%	11.23%	8.07%	7.49%
I_p (a.u.) ^c	298 K	18.45	101.61	125.19	156.91	231.03	261.78	297.27	212.96	208.57
	77 K	579.92	401.93	399.19	457.05	603.95	800.56	691.11	548.01	801.98
t (s) ^d	298 K	3.06	3.88	4.89	5.37	6.29	6.25	7.73	6.78	6.55

^a Phosphorescent lifetime monitored at 480 nm, λ_e : 280nm; ^b Phosphorescent quantum yield; ^c Phosphorescent intensity (λ_e : 280nm); ^d Time of ultralong luminescent intensity at 1 a.u.

table S3. Photophysical data of the PVA-100-3mg film at different temperatures.

System		293K	303K	313K	323K	333K	343K	353K	365K
τ_p (s) ^a	unirradiated ^c	0.32	0.26	0.24	0.2	0.15	0.09	0.05	0.04
	Irradiated ^d	0.74	0.72	0.68	0.63	0.56	0.47	0.36	0.27
I_p (a.u.) ^b	unirradiated	12.25	9.11	6.77	4.84	3.01	1.69	0.80	0.36
	Irradiated	349.34	317.58	287.74	265.53	237.82	193.79	138.48	83.73

^a Phosphorescent lifetime monitored at 480 nm, λ_e : 280nm; ^b Phosphorescent intensity (λ_e : 280nm); ^c Without 254nm UV irradiation; ^d 254nm UV irradiation for 65min.

table S4. Photophysical data of the PVA-100-3mg film at different excitation wavelengths under ambient conditions.

System		240nm	250nm	260nm	270nm	280nm	290nm	300nm	310nm	320nm
τ_p (s) ^a	unirradiated ^c	0.22	0.24	0.32	0.29	0.28	0.18	0.1	0.09	0.05
	Irradiated ^d	0.53	0.59	0.63	0.65	0.71	0.68	0.59	0.50	0.39
I_p (a.u.) ^b	unirradiated	10.11	--	14.84	--	17.87	--	10.92	--	2.21
	Irradiated	325.92	376.18	356.76	302.16	284.20	248.54	164.57	75.55	24.43

^a Phosphorescent lifetime monitored at 480 nm, λ_e : 280nm; ^b Phosphorescent intensity (λ_e : 280nm); ^c Without 254 nm UV irradiation; ^d 254nm UV irradiation for 65min.

movie S1. Appearance of the emitting G-doped PVA films when UV light is on and off.

movie S2. Appearance of the emitting PVA-100-3mg film when UV light is on and off.

movie S3. Imaging of the logo of the lotus flower.

movie S4. Imaging of the logo of the lotus flower containing AlQ₃.